UHV microscopy of the reconstructed Au(001) surface

D.N. Dunn, J.P. Zhang and L.D. Marks

Department of Materials Science And Engineering, Northwestern University, 2145 Sheridan Road, Evanston, IL 60208, USA

We investigate the microstructure of the reconstructed Au(001) surface using ultra-high vacuum transmission electron microscopy (UHV-TEM). Bulk single crystal Au(001) surfaces were prepared via standard metallographic techniques followed by repetitive cleaning of the surface with ion milling and annealing. After a clean surface was obtained, the (001) surface was found to reconstruct into two nearly orthogonal domains of dimensions $(5 \times n)$ where n ranges between 15 and 21. The unit cell vectors of the surface cell are parallel to the $\langle 110 \rangle$ directions of the unreconstructed fcc (001) surface. Analysis of the diffuse scattering and dark field micrographs indicates that the surface is sheared with a complicated domain and periodicity structure which depends upon the local geometry of the substrate.

1. Introduction

It has long been known that clean surfaces of Au will reconstruct into a variety of different surface configurations. The first evidence presented for the reconstruction of the Au(001) surface was given by Fedak and Gjostein [1], who found using LEED that it reconstructed into (5×1) surface cells. Several authors since then have investigated the Au(001) surface using LEED and found that it reconstructs into (5×1) [1,2], (5×20) [3–5] and $c(26 \times 68)$ [6] surface cells. Grønlund and Nielsen have found the Au(100) surface to reconstruct into two (5×20) orthogonal domains using RHEED [7], while Reider et al. found a (5×1) surface cell [8] using He diffraction techniques. More recently, a (28×5) reconstructed cell was found by Yamazaki et al. [9] for the Au(001) surface using ultra-high vacuum transmission electron microscopy (UHV-TEM). In most of the previous investigations of the reconstructed Au(001) surface some common elements appear. Firstly, in all but one [6] of the LEED studies above, one dimension of the reconstructed cell was found to be 5 times the bulk fcc spacing while the other dimension of the cell is always less precisely known. Also in most of the

models proposed to explain this reconstruction it is assumed that the reconstructed layer is hexagonal and has a spacing contracted from the bulk fcc (111) spacing [1]. It has also been pointed out by several authors [6,7,9] that the reconstructed Au(001) surface is not commensurate with the bulk lattice and is found in most cases to consist of domains rotated with respect to the bulk lattice. He diffraction and positive ion channeling spectroscopy (PICS) [10] have demonstrated that the reconstructed layer is on the order of a single monolayer in thickness.

It was thought early on that the surface reconstructed due to the segregation of impurities to the surface from the bulk [1,2]. This prompted subsequent studies of the clean Au(001) surface using AES to ensure the cleanliness of the surface being examined. The clean Au(001) surface was found to reconstruct into (5×20) surface domains while the (1×1) surface is found only when contamination is present [10]. Since much of the work to date on the Au(001) surface has been done using standard surface science techniques, relatively little has been said about the effect of bulk properties on surface reconstruction. Earlier work using UHV-TEM by Yamazaki and Takayanagi concentrated on thin film islands

of Au grown on a silver substrate. It is the intention of this paper to describe results using UHV-HRTEM on bulk Au(001) single crystal samples where the surface is found to reconstruct in the presence of a non-trivial concentration of bulk defects. In particular, we are able to explain different reports of the detailed structure of this surface as a consequence of different annealing and preparation conditions.

2. Experimental

All of the work presented in the following section was done on a Hitachi H-9000 ultra-high vacuum high resolution transmission electron microscope (UHV-HTREM). This microscope is a 300 keV microscope equipped with a Gatan parallel electron energy loss spectrometer (PEELS) and a base column pressure of 6×10^{-11} Torr with an attendant stable operating pressure of 2×10^{-10} Torr. Attached to the microscope is an ultra-high vacuum specimen transfer chamber (UHV-STC). The UHV-STC has a base pressure of $< 2 \times 10^{-10}$ Torr and is equipped with a Perkin-Elmer 4 keV ion gun, a Varian LEED - Auger unit, and a broad band optical annealing source capable of heating a metallic specimen to 600°C. This design allows one to prepare surface science specimens in the usual way, examine the specimen with surface sensitive techniques such as LEED and Auger spectroscopy (AES) and then have a look at the specimen in the microscope without changing the environment of the specimen and contaminating it.

Bulk Au(001) oriented single crystals were obtained from Atomergic Chemical Company and were spark cut into 3 mm disks. These disks were first mechanically polished using standard metallographic techniques and then dimpled so that the thickness at the dimple was 30 μm. These specimens were then cleaned and placed in the STC of the microscope where the crystal was sputtered with 4 keV xenon ions until transparent to 300 keV electrons. The crystal was then checked for contamination using PEELS and UHV-HREM. It was found with PEELS that after the initial ion milling with 4 keV xenon that

a significant amount of Xe had been implanted in the specimen causing line and point defects to appear in the bulk crystal. The specimen was then annealed until the xenon was no longer detectable to the PEELS and the bulk defect concentration had been reduced to acceptable levels.

The crystal was then cleaned with 2 keV Xe ions and annealed with the optical annealing source at 340°C. This process of sputter cleaning with low energy Xe ions and annealing was repeated until a clean, well ordered, (001) reconstructed surface was obtained. Once the reconstruction was established, the surface was re-cleaned and re-annealed for varying times to investigate the effect of annealing on the material. The evolution of the microstructure during annealing has been reported elsewhere.

3. Results

We will break up the results into a discussion of the basic features of the reconstructed gold (001) surface, followed by an analysis of the domain structure. These two will be tied together in the discussion section where we show that the large variation in results can be understood within a simple model based upon local variations in the bulk strain fields.

3.1. Basic crystallography of the reconstruction

Before describing the various forms of the reconstruction that were observed, it is important to detail the basic elements. We will first discuss the diffraction pattern shown in fig. 1. The background in all cases is a bulk (001) crystal which produces a square reciprocal lattice mesh with diffuse structure in the diffraction pattern arising from bulk defects. In addition to the bulk spots, diffraction from the surface mesh (e.g., {110} diffraction spots) is also present in the diffraction patterns. It is important to recognize that these spots are due to an incomplete number of (001) layers along the beam direction and as such are *both* bulk and surface sensitive; a bulk defect can lead to an incomplete number of layers as readily

as, for instance, a surface step. Analysis of dark field images using bulk {200} spots indicates the presence of voids in the material (e.g., fig. 5c), and the square nature of the (002) and (022) spots in fig. 2 implies that the voids are tetrahedrally shaped. The shape of the bulk (110) spots depends upon the concentration of voids and, in fig. 1 for instance, the (110) spot is very diffuse.

Superimposed on this bulk diffraction is far weaker surface diffraction from what initially appears to be two but is in reality four different domains; we will leave for later the exact analysis in terms of the four domains and just deal with two 90 degree rotation domains. Each of these domains corresponds to an hexagonal mesh corresponding to a single (111) monolayer contracted by about 4% with respect to the normal bulk (111) spacing. The contraction can be best seen by noticing that the two additional surface spots between the bulk (200) spots are not collinear, but lie slightly above a line connecting the bulk spots. We should also note that the diffraction pattern is consistent with monolayers; if there were more than one layer of (111) mate-

Fig. 2. Shown are the low index diffraction spots from the reconstructed Au(001) surface. The squared shape of the spots correlates well with the presence of tetrahedrally shaped voids in the bulk crystal which are remanents from the ion milling stage of surface preparation.
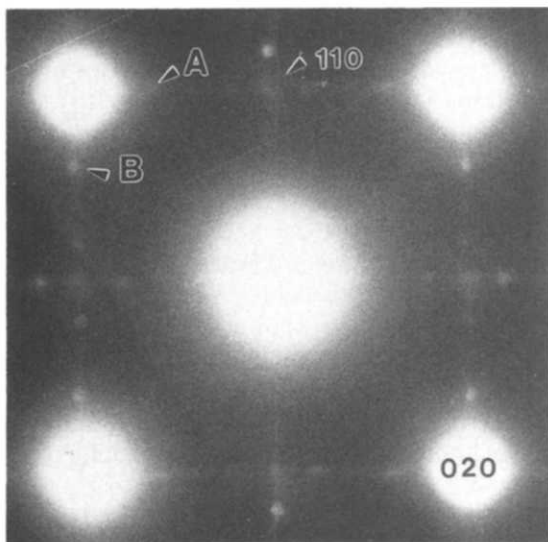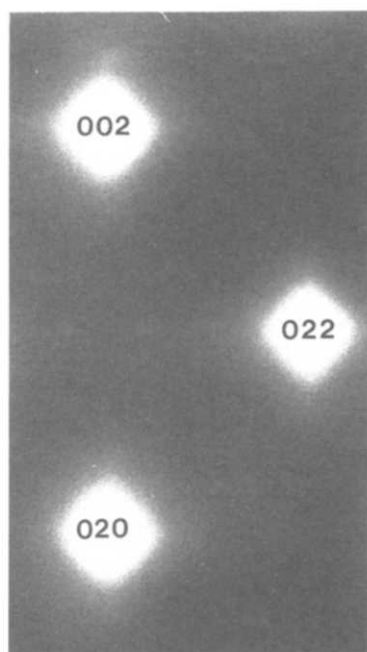

Fig. 1. An early stage diffraction pattern showing all of the general features exhibited by the reconstructed Au(001) surface reconstruction. A and B demarche satellite spots from the reconstructed surface and a surface {110} type spot is also marked.

rial stacked either as hcp or fcc the surface structure factor would be very different, and furthermore the intensities of the surface spots were consistent with a single monolayer on the top and bottom surfaces. In addition there are additional spots which can be attributed to some combination of double diffraction between the surface and bulk and, in principle, a modulation of the bulk material. The modulation that we are referring to would be the strain field associated with the surface reconstruction. In terms of a coincident site lattice between the bulk and surface, there is a strong coincidence along one bulk (110) direction of 5 and approximately a 20 coincidence normal to this; we will describe this as a $5 \times n$ structure and later refer to the "5" and "n" directions for more detailed analysis.

The basic imaging technique that we have used is dark field imaging with an objective aperture around different diffraction spots. The objective aperture used was of a size that did not allow a

single spot to be used so that typically, a bulk spot and two or three satellite spots were used in taking the dark field images. The most important dark field images were taken with the bulk {002} type spots with the surface satellite spots shown in fig. 1 included within the aperture. This gave images where the interference between the bulk and surface spots shows the local orientation of the "5" period of the domains, see fig. 3b. In other cases, dark field using bulk {022} spots produces constrast from the "*n*" dimension of the reconstructed domains as will be discussed further below.

Let us now return to the full breakdown of the diffraction pattern into four different domains. Closer analysis of the diffraction pattern indicates that the spots between a pair of bulk (200) spots are split into two, see fig. 3a. It is significant to

note that the spot along the bulk (110) direction showed in general a far smaller (if any) splitting. Previous analyses of this surface have reported a rotation of the domains by about 0.5 degrees leading to a breakup into four domains. However, a rotation would lead to equal splitting of all diffraction spots and this is not the case. We can therefore conclude that the breakdown into four domains is due primarily to a shear normal to a bulk (110) direction, i.e., normal to the "5" direction. The presence of the four domains can be readily seen in {200} dark field images, for instance fig. 3b.

To summarise the general features of the reconstruction, there exists a surface hexagonal monolayer with a surface mesh contracted by about 4% relative to a bulk (111) gold layer which approximately fits on the surface with a $5 \times n$
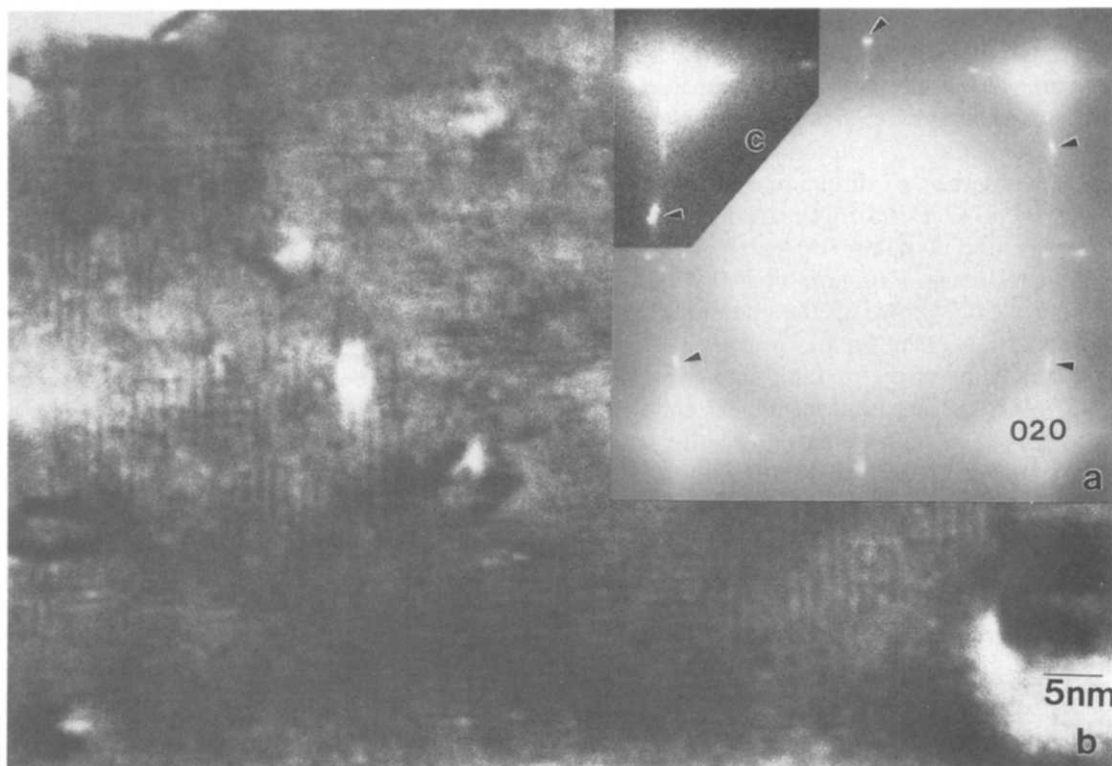

Fig. 3. (a) Diffraction pattern showing the splitting of satellite spots around the (200) diffraction spots where the split spots are indicated with arrows. (b) A dark field image using the bulk (200) spot as well as the associated reconstruction satellite spots which shows the presence of four domains. (c) A blow up of a (200) type bulk spot with the associated split satellite spots.

coincident site lattice. However, there are many more details about the surface which we will discuss further below.

3.2. Domain structure

There is a vast amount of fine detail in both the images and diffraction patterns which indicates that the domain structure of the reconstruction is in fact exceedingly complicated. We should mention that other surfaces which we have looked at, for instance the boron doped Si(111)$\sqrt{3} \times \sqrt{3}$ R30° [11–13] such detail was missing so this is not an artifact of electron microscopy. The first point to mention is that there is a substantial amount of diffuse scattering along the "5" direction around the surface spots which depends upon the exact annealing treatment of the material. Fig. 4 shows a montage of diffraction patterns concentrating on this region as a function of improving annealing of the material. To assist in interpretation of this diffuse scattering, fig. 5 shows a comparable montage of {200} images. In the earlier micrographs in figs. 4 and 5 the domain size along the "5" direction is small but quite large along the "n" direction. In particular, a common occurrence is an intimate intergrowth of pairs of sheared domains, see fig. 5a. This may be just a microdomain structure, or it may in fact be a stable modification of the material by a constant shear wave (see fig. 6).

As the annealing of the material improves, the bulk {110} spots become sharper, consistent with both the removal of bulk defects and better flatness of the surface. However, there is no noticeable difference in the overall film uniformity as the annealing improves so we are led to believe that the major difference is the reduction in the number of bulk defects and associated strain field. The only change in the surface structure is growth in the size of the reconstructed domains and a reduction in the amount of diffuse scattering, see for instance figs. 4c and 5c. As the annealing improves the splitting of the spots in each pair of domains becomes more apparent and can be seen more clearly further out in the diffraction pattern, see for instance fig. 4d.
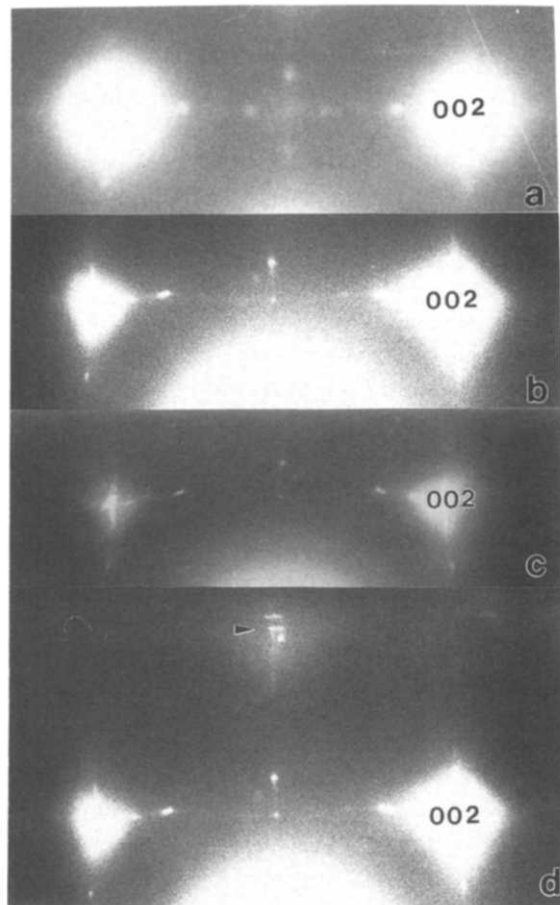

Fig. 4. Shown here is a montage of diffraction patterns as a function of annealing time. (a) Diffraction pattern showing the (200) spots and surface spots for the early stage of the reconstruction. It should be noted that the diffraction pattern is sensitive to the evolution of the reconstruction as is shown by the small difference between the background and surface spot intensities. (b) Shown is an off the zone axis diffraction pattern after more annealing. The diffuse intensity between the (200) spots is decreased and the intensity of the surface spots is increasing. The satellite spots near the (200) bulk spots are beginning to split. (c) Shown is an off the zone axis diffraction pattern exhibiting a marked decrease in diffuse scattering and splitting of satellite spots near the (200) spots. The intensity of the surface spots is increasing indicating an ordering of the reconstruction. (d) An off the zone axis diffraction pattern after still more annealing showing the spitting of the satellite spots near the (200) bulk spots. The spot splitting can be seen more clearly in the (220) type diffraction spot which is arrowed.

In addition to these changes to the domain structure, there are substantial variations in the "n" coincidence. In the less well annealed samples, this was quite difficult to observe and only

'5' Fringes of The (5xn) Reconstruction

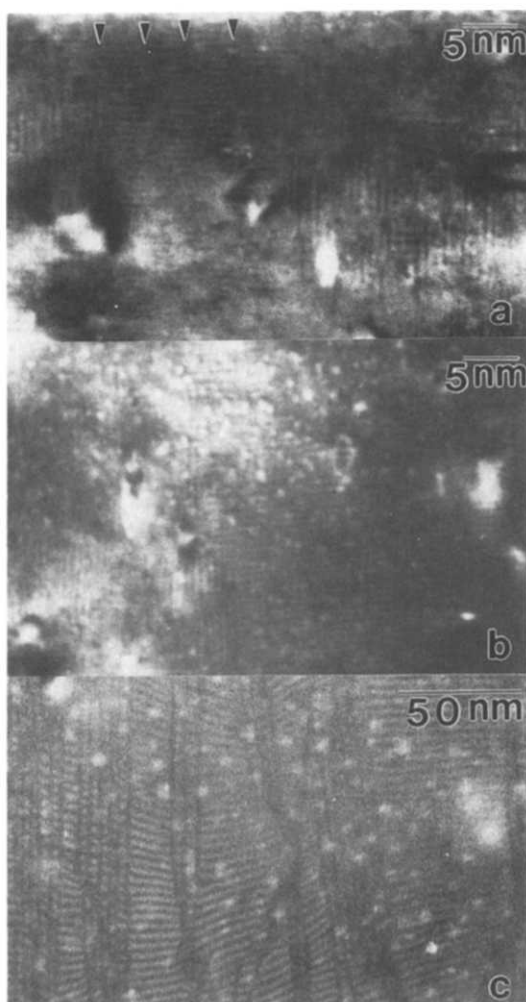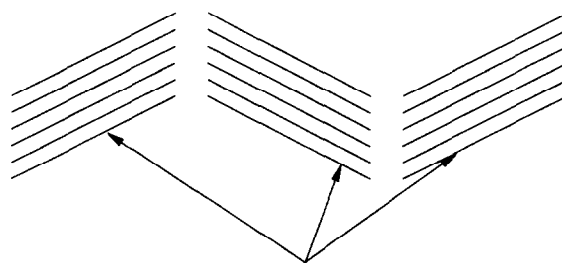Fig. 6. A schematic diagram of a possible shear structure shown in fig. 5a.

Fig. 5. Shown here is a montage of dark field images taken with (200) and surface satellite spots. (a) Shows the intimate intergrowth of pairs of sheared domains. This modulation may be due to a shear wave along the longer dimension of the reconstructed surface cell. Arrows indicate the units of the shear modulation. See fig. 6 for a probable shear structure. (b) Dark field image showing clear domain structure as well as the presence of voids which are left over from the ion milling process. These voids are responsible for the diffuse scattering seen in the diffraction patterns as shown in fig. 4. (c) A dark field image taken with the (200) and satellite spots showing several domains of different sizes and shapes.

with longer annealing did it become more apparent. With the latter samples it was quite clear that the "n" coincidence was not a fixed number but, in fact, varied from domain to domain and even within domains. For instance, fig. 7 shows a region where a number of domains are visible with slightly different orientations and in some cases small changes in the apparent periodicity at the edge of the domain. It is very dangerous to directly interpret these spacings since local strains can couple into the apparent spacing observed, but they do indicate local variations. We should also note that the domains do not appear to cross the line where a dislocation (arrowed) is passing within the bulk. A clearer demonstration of the local variations is shown in the high resolution images shown in fig. 8 where both the "5" and the "n" dimension can be resolved. Whereas the "5" dimension does not vary, it is clear that the "n" dimension of the structure is very different.

4. Discussion

All the above information appears to be very complicated, but in fact can be understood relatively easily; in the process it becomes apparent why there has been so much discussion in the literature of the fine details of the reconstruction but agreement about the basic elements. First, we should state that the *average* structure of the reconstruction is a 5×20 cell; this agrees with the previous work and does not appear to change substantially. Our only disagreement is that the
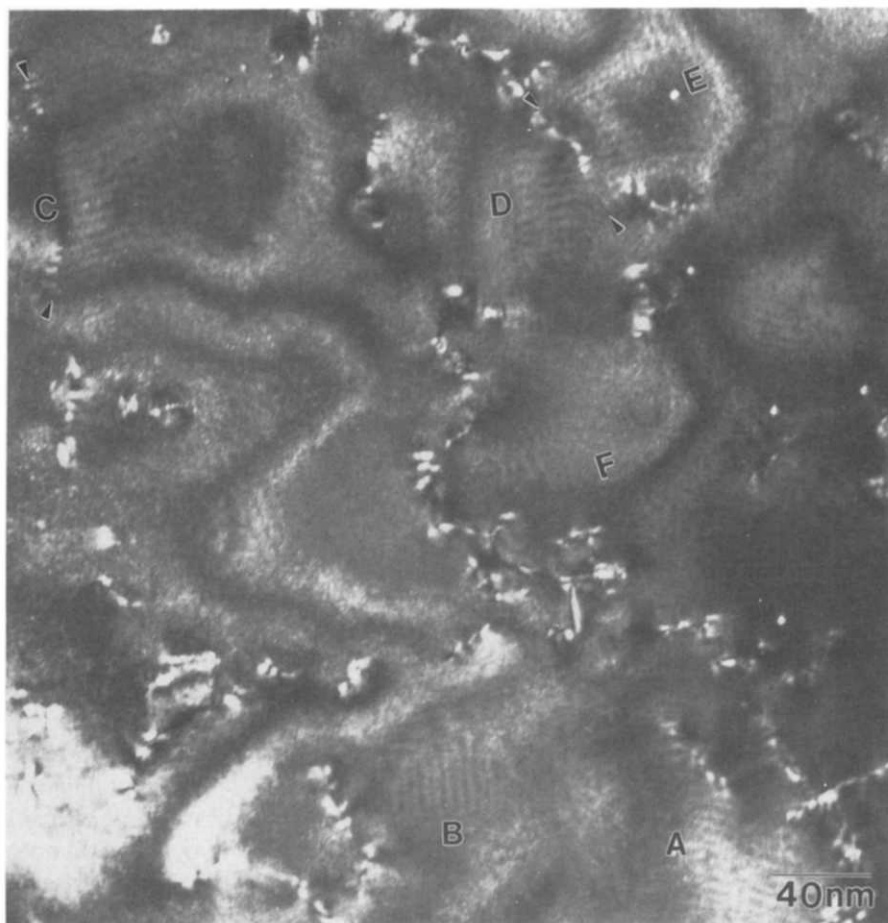
Fig. 7. A dark field image taken with the (220) and surface satellite spots showing the existence of several domains. These domains are marked A through F and are oriented along several directions. Closer examination reveals that these domains are clearly confined by the presence of dislocation lines near the surface which are arrowed.

material is sheared, not rotated; however, since this conclusion concerning rotation came from small plate like crystallite samples [9], surface effects may be responsible for the differences seen here.

A significant feature of the reconstruction is that the "5" coincidence is strong and does not appear to substantially change. Looking at the coincidence between the surface and bulk as sketched in fig. 9, it is apparent that there are regions of excellent matching along this direction which will tend to lock the surface layer with respect to the bulk. If the surface is sheared normal to this layer, there will be relatively little

change in the total energy. We find it useful to think of the "5" direction as a hard direction, and the "n" direction as soft.

The variations in the "n" dimension can be understood as local accommodations to strains. High resolution electron microscopy and ion channeling data indicates the presence of a substantial buckle along the "5" direction which would lead to a significant bulk strain field. In a large domain the center will approach one value of the "n" component, but at the edges or when the substrate geometry changes the strain field will change which explains the local variations shown in figs. 7 and 8. This is also consistent with
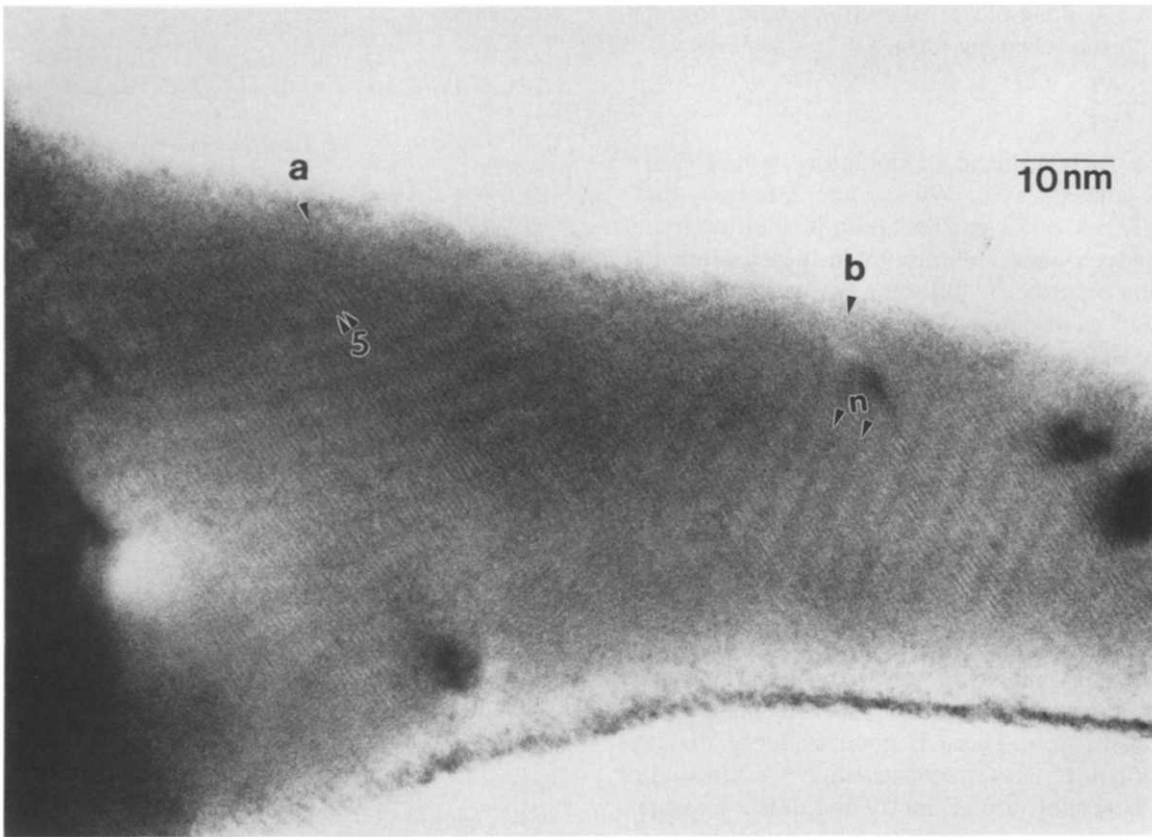
Fig. 8. A high resolution image showing both the "5" and "n" dimension of the reconstructed surface. The "5" dimension is seen to be a hard dimension while the "n" dimension is seen to have a wavy character. There is a noticeable switch in orientation of the reconstructed domains marked by a and b as a function of distance along the peninsula shown in the image.

the fact that the domains do not appear to cross the strongly strained region near to dislocations.

To summarize the above, the nature of the reconstruction on gold (001) is a hexagonal mono-layer which is easily locked in along the "5" direction. The exact nature of the "n" component depends heavily upon the local geometry and local strain. The data is consistent with a shear of
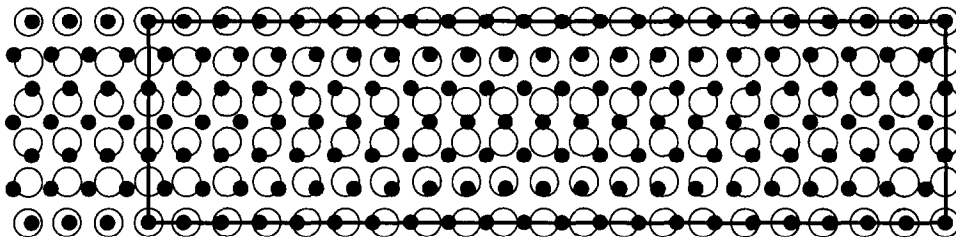

Fig. 9. A coincident site lattice construction of the $(5 \times n)$ reconstructed surface. Coincidence for the "5" dimension is very strong and should tend to lock the surface layer along this dimension. This dimension is then referred to as a hard dimension while the "n" dimension exhibits no similar locking tendency. It is possible that with the appropriate strain along the (011) directions to make the n dimension range from 15 to 22.

about 1% along the "5" direction leading to a cell of with the following form,

$$\begin{bmatrix} 5 & 0 \\ \delta n & n \end{bmatrix},$$ (1)

as the "best" coincident site lattice, where $15 \leq n \leq 21$ and $\delta = 0.01$. We cannot, however, completely rule out a small rotation in addition to the shear seen above. Variations in the experimental results reported by different groups can be rationalized as variations in the exact nature of the surface since they were not able to determine directly the defect structure beneath the surface (e.g., dislocations, point defects).

To summarize, clean Au(001) surfaces were prepared under UHV conditions and the surface reconstruction was followed using transmission electron diffraction and conventional TEM imaging methods. The clean surface reconstruction of a Au(001) surface was found to reconstruct into nearly orthogonal $(5 \times n)$ domains, where n is between 15 and 21. These domains are sheared by 0.5 degrees along the "5" directions of the reconstruction. There is good evidence that the exact nature of the reconstruction is a function of the local substrate geometry and defect locations.

References

[1] D.G. Fedak and N.A. Gjostein, Acta Metall. 15 (1967) 827.

[2] D.G. Fedak and N.A. Gjostein, Phys. Rev. Lett. 16 (1966) 171.

[3] D.G. Fedak and N.A. Gjostein, Surf. Sci. 8 (1967) 77.

[4] P.N.J. Dennis and P.J. Dobson, Surf. Sci. 33 (1972) 187.

[5] G.E. Rhead, J. Phys. F 3 (1973) L53.

[6] M.A. Van Hove, R.J. Koestner, P.C. Stair, J.P. Biberian, L.L. Kesmodel, I. Bartos and G.A. Somorjai, Surf. Sci. 103 (1981) 189.

[7] F. Grønlund and P.E. Hojlund Nielsen, J. Appl. Phys. 43 (1972) 391.

[8] K.H. Reider, T. Engel and R.H. Swendsen, Surf. Sci. 127 (1983) 223.

[9] K. Yamazaki and K. Takayanagi, Surf. Sci. 199 (1988) 595.

[10] D.M. Zehner and B.R. Appelton, J. Vac. J. Technol. 12 (1975) 454.

[11] P. Bedrossian, R.D. Meade, K. Mortensen, D.M. Chen, J.A. Golvochenko and D. Vanderbilt, Phys. Rev. Lett. 63 (1989) 1257.

[12] R.L. Headrick, I.K. Robinson, E. Vlieg and L.C. Feldman, Phys. Rev. Lett. 63 (1989) 1253.

[13] S. Bensalah, J.P. Lacharme and C.A. Sébenne, Surf. Sci. 211/212 (1989) 588.